SUPPORTING INFORMATION

Membraneless Electrolyzers for the Simultaneous Production of Acid and Base

Oyin Talabi[1], Anna Dorfi[2], Glen O'Neil[2], Daniel V. Esposito[2,*]

[1] Department of Chemical Engineering, Loughborough University, Loughborough, Leicestershire, LE11 3TU, UK
[2] Department of Chemical Engineering, Columbia University, 500 W 120th St, New York, NY 10027, USA
*de2300@columbia.edu

Table of Contents

I. Materials and Methods

1.1 Chemicals

All solutions were prepared using 18.2 MΩ-cm deionized water. Concentrated sulfuric acid (Certified ACS plus, Fischer Scientific), sodium sulfate (ACS Reagent grade, Sigma Aldrich), potassium tetrachloroplatinate (99.99% trace metals basis, Sigma Aldrich) and potassium nitrate

(ReagentPlus 99.0%, Sigma Aldrich) were used as received without further purification. The pH of the Na_2SO_4 electrolyte (initially pH≈ 5) was adjusted to pH=7 by titrating with 1 M NaOH.

1.2 Electrode Fabrication

Both anode and cathodes were made from titanium mesh (80 mesh; 130 µm wire diameter, Alfa-Aesar) that was platinized as described below in a solution of 3 mM K_2PtCl_4 and 0.5 M NaCl (ACS Reagent Grade, Calbiochem®). Before platinization, titanium mesh electrodes were first subjected to a pre-treatment involving double-step chronoamperometry in 0.5 M H_2SO_4, with an applied potential of -2 V to 2.5 V for one minute. Platinum electrodeposition was then carried out by means of cyclic voltammetry (CV), with the applied potential cycled 20 times between 0.3 and -0.7 V vs. Ag/AgCl, using a scan rate of 100 mV s^{-1}, in a solution of 3 mM K_2PtCl_4 and 0.5 M NaCl (pH = 3.1). The total duration for the electro-deposition of each electrode was approximately five minutes.

1.3 Electrolyzer Fabrication

The body of the membraneless electrolyzers was fabricated from natural color poly (lactic acid) (PLA) filament using a MakerBot replicator 2.0 3D printer (MakerBot Industries). A schematic exploded view of the cell is provided in Figure S1. The electrolyzer design was made in AutoDesk Inventor Professional CAD software, and the design files are available for free download at echem.io. The cell was 3D printed with a 0.1 mm layer height and a 15 % infill. The fluidic channel of the flow cell was 7.0 cm long, 1.3 cm wide and 0.5 cm high, with a 3.3 cm by 0.1 cm product divider placed downstream of the electrodes. The cross-section of each product channel was 0.5 cm x 0.6 cm, and the I.D. of the inlet and outlet connection tubes were 4.0 mm. The electrolyzer was assembled by positioning two platinized titanium mesh electrodes at a 180° angle to each other within the printed flow cell. The Pt/Ti mesh electrodes and glass windows

(for visualizing electrolyzer operation) were epoxied to the cell body using JB Weld 5-minute epoxy and given at least 24 hours to set.

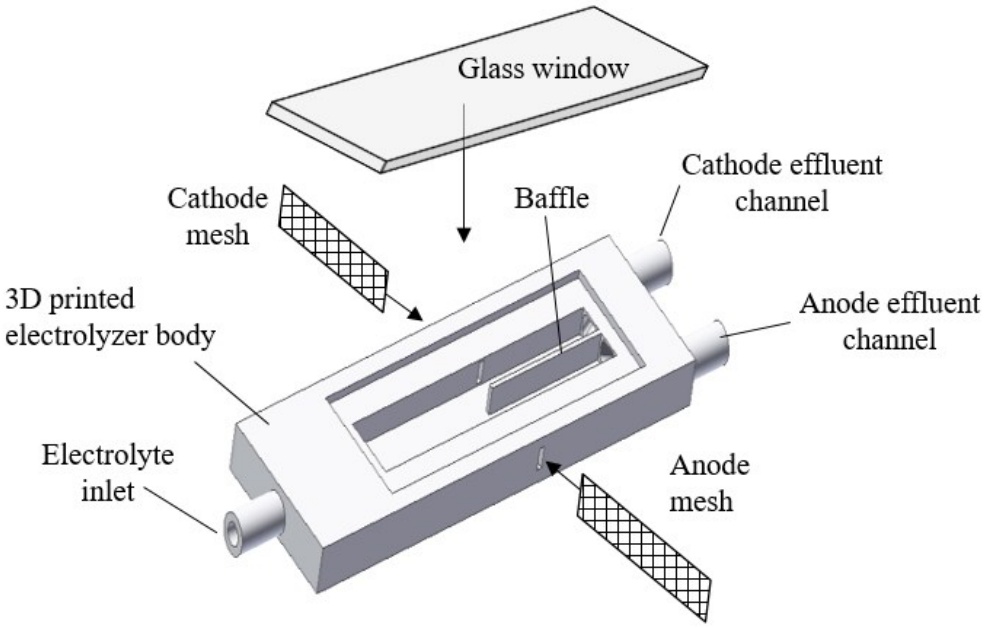

Figure S1. 3D exploded view of the membraneless electrolyzer used in this study.

1.4 Experimental Set-ups

All experiments were performed using a Biologic SP-300 or SP-200 potentiostat. The performance of individual electrodes (3-electrode measurements) and electrolyzers (2-electrode measurements) were evaluated using cyclic voltammetry (CV) or linear sweep voltammetry (LSV). 3-electrode CV curves for the Pt/Ti electrodes were evaluated in a glass, 3-neck electrochemical cell. All three electrode measurements employed Ag|AgCl reference electrode (REF321, Hach), and a graphite rod as the counter electrode.

The experimental set-up used to evaluate the performance of the membraneless electrolyzer devices is shown in Figure S2. The pH 7 aqueous brine solution was first loaded into a ≈1 L reservoir with an air tight screw cap. One piece of flexible PVC tubing (McMaster-Carr)

was secured to a port connected to the headspace the reservoir, while the other end of the tubing was placed in the pump head of a Cole Parmer Masterflex L/S peristaltic pump. A second piece of PVC tubing was used to connect the inlet port of the membraneless flow cell to a port located at the bottom of the reservoir. When the pump was turned on, laboratory air was pumped into the headspace of the brine reservoir, creating pressure in the air-tight vessel that caused the brine solution to flow into the inlet channel of the horizontally mounted membraneless electrolyzer. The volumetric liquid flow through the set-up was directly measured for different rotational speeds of the peristaltic pump. This method of pressure-induced fluid flow was used instead of directly pumping the liquid electrolyte because it was found to be much more effective at dampening noise associated with the pulsating nature of the fluid flow that is naturally created by the peristaltic pump.

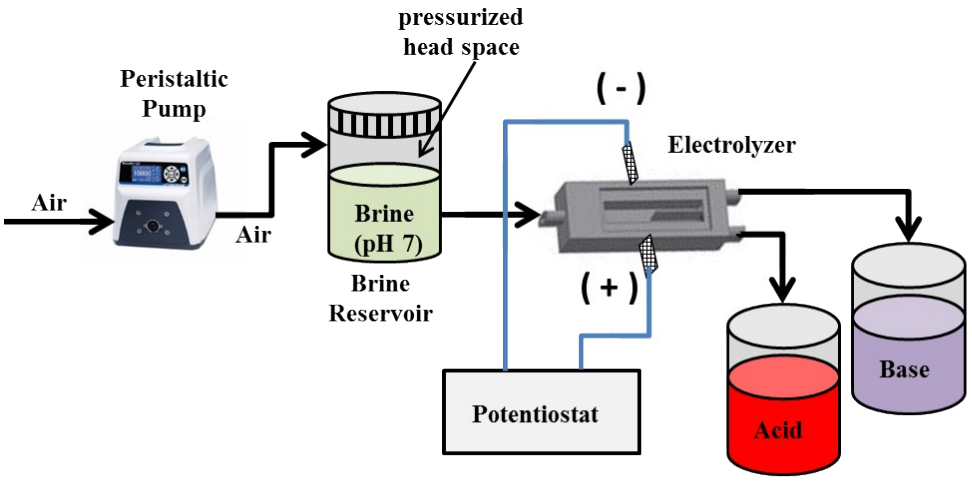

Figure S2. Process flow diagram for membraneless flow cell set-up used to produce acid and base of varying concentrations.

1.5 Product Collection and Analysis

During operation of the flow-cell set-up, the flowing electrolyte forces the electrolysis products to flow down the anode and cathode effluent channels, which are separated from each other by a

1 mm thick insulating divider that is part of the cell body. Upon exiting the flow cell, the product streams were collected in glass beakers that were placed directly below the outlets of the flow cell. The split in fluid flow between the two effluent channels was typically close to even, with the average difference in liquid volume collected in the anode and cathode product collection beakers being 12 % across all experiments. Chronopotentiometry (CP) electrolysis experiments were performed at constant applied current densities of 4.2 mA cm^{-2}, 10.4 mA cm^{-2}, 20.8 mA cm^{-2}, 41.7 mA cm^{-2}, 104.2 mA cm^{-2}, and 208.3 mA cm^{-2}. After allowing the electrolysis experiment to reach steady state operation (≈60 s), 20-25 mL (pH probe measurements) or 35-50 mL (titration measurements) of product solution was collected in each of the two collection beakers. The pH values of the collected product solutions were measured using a Fisher Scientific Education bench-top pH meter (Model pH 510), which was calibrated with commercial pH 4.01, 7.00 and 10.01 buffer solutions (Oakton). For pH probe measurements of effluent pH, every electrolysis experiment was performed twice, and the average of the two pH values for each product stream is provided in Figure 3 of the main article.

In order to more accurately measure current utilization at the anode and cathode, an additional series of experiments were performed where the amount of acid/base generated during electrolysis was determined by acid-base titration. These experiments were conducted at constant current densities of 41.7 mA cm^{-2}, 104.2 mA cm^{-2}, and 208.3 mA cm^{-2} for a constant net electrolyte flow rate of 0.62 mL s^{-1}. In these measurements, the collected cathode and anode effluent solutions were neutralized by titrating them with known concentrations of base (0.005 M KOH or NaOH) or acid (0.005 M HNO_3 or H_2SO_4), respectively. Before titrations, two to three drops of a phenol red (Valterra Products) pH indicator dye were added to the collected effluent (the titrand) and allowed to thoroughly mix throughout the solution. The color of this dye is most

sensitive between pH 6 and pH 8, and was used to visually observe when the solution became neutralized. The titration was performed while actively mixing the solution, and the volume of the titrant was recorded when the pH dye indicator turned a bright orange (indicating pH 7) and when the pH probe read 7. After completing the titration experiment, the moles of titrant needed to reach neutralization (pH=7) was used to calculate the number of moles of H^+ (anode effluent) or OH^- (cathode effluent) that were present in the collected effluent solutions. Additionally, control solutions comprised of varying concentrations of acid (HNO_3 or H_2SO_4 in 1 M KNO_3 or 1 M Na_2SO_4, respectively) or base (KOH or NaOH in in 1 M KNO_3 or 1 M Na_2SO_4, respectively) were synthesized and titrated in the identical manner as the electrolysis products. These control experiments were used to determine the molar ratio of titrant to titrand required to neutralize the solution, information that was in turn used in calculating the moles of H^+ or OH^- generated in the electrolysis experiments based on the moles of titrant required to neutralize the solution. Dividing the moles of H^+ or OH^- generated by the volume of the collected effluent solution allowed for determination of $[H^+]$ and $[OH^-]$ of these solutions, values which were used to compute the current utilization at the anode and cathode as described in Section IV.

II. Electrochemical Characterization of the Pt/Ti Mesh Electrodes

Electrochemical characterization of the platinized Ti electrodes was performed by conducting cyclic voltammetry (CV) in three different electrolytes: 1 M H_2SO_4, 1 M Na_2SO_4 (adjusted to pH 7) and 1 M KNO_3 (pH 7). 3-electrode CV curves are provided in Figure S3a, where the current density is normalized to the 2-D area of the mesh electrode, and the potential is given versus the reversible hydrogen electrode (RHE) in order to provide a comparison of the onset potentials for the OER and HER in each electrolyte. In all electrolytes, the exponential rise in current at

positive potentials is associated with the OER, while the sharp decrease in current at negative potentials near the lower scan vertex results from the HER. As discussed in the main article, some of the oxidation current in the Na_2SO_4 solution may result from the oxidation of sulfate ions to persulfate ions. The reduction features visible in between the OER and HER onset potentials are associated with Pt-oxide reduction, reduction of O_2 that was evolved near the positive vertex, and underpotential adsorption of hydrogen.

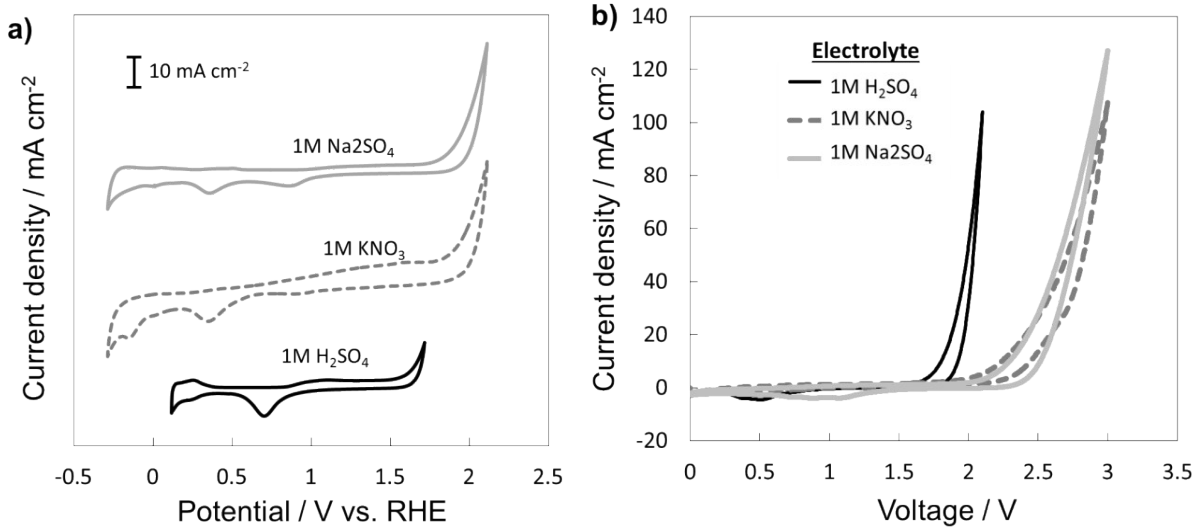

Figure S3 a.) 3-electrode and b.) 2-electrode cyclic voltammograms measured with platinized Ti mesh electrodes in 1 M H_2SO_4, 1 M KNO_3 (pH=7), and 1 M Na_2SO_4 at 100 mV s^{-1}.

The performance of the Pt/Ti electrodes for brine electrolysis was also evaluated by measuring current density-voltage (JV) curves in a symmetric two electrode arrangement in which identical Pt/Ti mesh were used for both the anode and cathode (Figure S3b). Consistent with the 3-electrode CV measurements, the 2-electrode JV curve measured in 1 M H_2SO_4 has a significantly lower onset voltage for electrolysis (≈ 1.68 V) compared to those observed in the 1 M KNO_3 (≈ 1.95 V) and 1 M Na_2SO_4 (≈ 2.10 V) solutions. These values of the onset voltages were evaluated at a current density of 3 mA cm^{-2}. Additionally, the slopes of the JV curves in the

neutral salt solutions are slightly smaller than that recorded in the 1 M H_2SO_4 solution. This observation can be attributed to a lower conductivity of the pH neutral brine solutions compared to the H_2SO_4, as well as a Nernstian penalty associated with the local changes in pH near the electrode surface.

The two electrode JV curves can be used to estimate the molar electrical energy input (E_e) required to produce the acid and base products by dividing the electrical power based on the operating current (I) and voltage (V), $P_e=I\cdot V$, by the molar rate of acid and base production based on Faraday's law:

$$E_e = \frac{I \cdot V}{\left(\frac{I \cdot \xi_{OH-}}{n_c \cdot F}\right) + \left(\frac{I \cdot \xi_{H+}}{n_a \cdot F}\right)} = \frac{F \cdot V}{\left(\frac{1}{n_c} + \frac{1}{n_a}\right)} \quad \text{(S1)}$$

where F is the Faraday constant, n_c is the electron transfer number for the production of base at the cathode, n_a is the electron transfer number for the production of acid at the anode, and ξ_{OH-} and ξ_{H+} are the current utilization at the cathode and anode, respectively (see Section IV for detailed discussion on current utilization). If $\xi_{OH-}= \xi_{H+}=1$ and $n_c=n_a=n$, then Equation (S1) simplifies to Equation (S2):

$$E_e = \frac{n \cdot F \cdot V}{2} \quad \text{(S2)}$$

Using the applied voltage from the 2-electrode JV curves at a current density of 100 mA cm^{-2}, the electrical energy per mole of HNO_3 and KOH produced from the electrolysis of HNO_3 is computed from Equation (S2) to be equal to 0.08 MWh·$kmol^{-1}$. It must be emphasized that this value represents the electrical energy required to produce the acid and base product, and does not include the energy that may be required to concentrate and/or purify the product.

III. Activity Coefficients used to Calculate Modeled Effluent pH

The pH of the effluent streams was modeled as a function of applied current density using Equations (5) and (6) from the main text. Activity coefficients for H^+ in the anode effluent and OH^- in the cathode effluent were calculated as follows. First, the mean activity coefficients ($\gamma_\pm$) for HNO_3 ($\gamma_{\pm,HNO3} = 0.791$) and KOH ($\gamma_{\pm,KOH} = 0.798$) were taken from literature for a temperature of 25 °C and a molality of ≈ 0.1 mol kg^{-1}.[1] Individual activity coefficients (γ_i) for K^+ and NO_3^- were also obtained from literature and found to be $\gamma_{K+} = \gamma_{NO3-} = 0.74$ at 25 ^{0}C and for the same ionic strength (1 molal) as cited above.[2] The activity coefficients for H^+ in an acidic KNO_3 solution and OH^- in an alkaline KNO_3 solution were then calculated from Equation (S3):

$$\gamma_\pm = \sqrt{\gamma_+ \gamma_-} \tag{S3}$$

where $\gamma_\pm$ is the mean activity coefficient for a univalent electrolyte, and γ_+ and γ_- are the activity coefficients for the cation and anion species, respectively. Using Equation S4 and the activity coefficient values from literature, it is estimated that γ_{H+}=0.85 and γ_{OH-}=0.86. The value of γ_{H+}=0.85 is identical to the value of γ_{H+} reported in another independent reference for γ_{H+}=0.85 in a KOH solution at the same molality and temperature.[3]

IV. Current Utilization Plots

The current utilization, ξ, is defined as the ratio of the experimentally observed rate of H^+ or OH^- generation to the rate of generation of those species that should be theoretically observed based on Faraday's law. ξ can be thought of as a Faradaic efficiency for the production of OH^- at the cathode and H^+ at the anode. ξ for the anode and cathode streams were calculated from Equations (S4) and (S5), respectively:

$$\xi_a = \frac{[H^+] \cdot (v/2)}{J \cdot A/(n \cdot F)} \quad \text{(S4)}$$

$$\xi_c = \frac{[OH^-] \cdot (v/2)}{J \cdot A/(n \cdot F)} \quad \text{(S5)}$$

where (v/2) is the volumetric flow rate through one effluent channel, J is the average current density, A is the area of a single electrode, F is the Faraday constant, and n is the electron transfer number (mole e^- per mole OH^- or H^+). For both the HER and OER reactions provided in Equations (1) and (2) of the main article, respectively, n=1. Equations (S4) and (S5) assume that the starting pH of the brine is neutral such that the generated [H^+] and [OH^-] are much greater than 10^{-7} M. [H^+] and [OH^-] were determined from the acid-base titration experiments, as described in Section III of this document. The resulting values of ξ_a and ξ_c determined from acid-base titration analysis of the effluent product from KNO_3 and Na_2SO_4 are provided in Figure S4. In all cases, relatively high current utilization values are observed for both brine solutions, although ξ_a and ξ_c were found to be consistently lower for KNO_3.

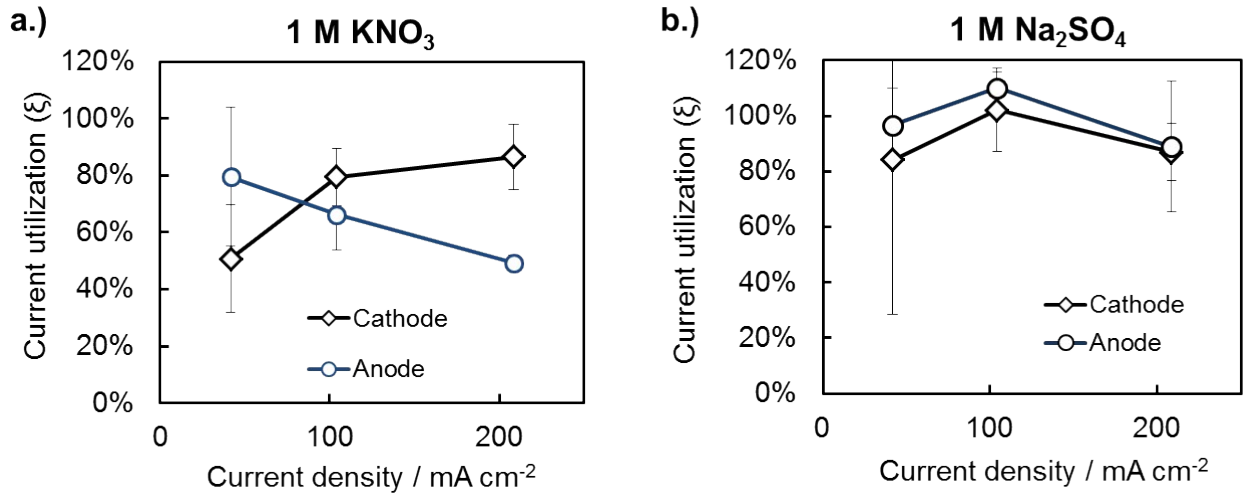

Figure S4: Calculated current utilization curves for a.) the production of acid at the anode and b.) the production of base at the cathode of the membraneless electrolysis. Values of current utilization were computed as described in the text based on acid-base titration analysis of the collected anode and cathode effluent streams. Each of the current utilization values provided in

this plot are average values that were determined from 3 or 4 repeated electrolysis experiments, and error bars are based on 95% confidence intervals.

V. Buffer Effect of Sulfate Anions on Cathode Effluent pH

In Figure 3c of the main article, it was noted that the measured pH of the acidic anode effluent produced from Na_2SO_4 electrolysis was significantly higher than the anode effluent stream from KNO_3 electrolysis and the pH expected from Equation (5) (with ξ_a=1). A higher than expected anode effluent pH could be explained by low ξ_a, but acid-base titration analysis of the anode effluent (Fig. S4b) indicate that this is not the case. Instead, the most likely cause of the significantly higher than expected pH for the anode effluent during Na_2SO_4 electrolysis is a buffering effect associated with sulfate ions. This is shown by the reverse reaction:[4]

$$SO_4^{2-} + H^+ \leftrightarrow HSO_4^- \tag{S6}$$

The pK_a corresponding to the acid dissociation constant (K_a) for this reaction is 1.99 at 25 °C. In the Na_2SO_4 electrolysis experiments, the production of excess H^+ at the anode results in a shift in the chemical equilibrium to the right, with a portion of the H^+ reacting with free sulfate ions to form HSO_4^-. Thus, the concentration of free H^+ is equal to that predicted from Equation (3), minus that which reacts with SO_4^{2-} according to Equation (S6). In order to calculate the equilibrium $[H^+]$, one must also account for the reversible reaction between SO_4^{2-} and Na^+:

$$SO_4^{2-} + Na^+ \leftrightarrow NaSO_4^- \qquad K_{eq} = 0.24 \tag{S7}$$

for which the equilibrium constant is K_{eq} = 0.24.[5] At equilibrium, the $[H^+]$ can be calculated by simultaneously solving the equilibrium relations associated with Equations (S6) and (S7) based on the initial concentration of Na_2SO_4 (1 M) and the number of moles of H^+ generated from electrolysis (Eqn. (3)). The predicted pH of the anode effluent, buffered by the presence of the

sulfate anions, can then be calculated from the equilibrium value of $[H^+]$ as a function of J. By this means, the pH in the buffered solution was modeled as a function of J, and the result is shown in Figure S5 (solid line) along with the modeled anode effluent pH in the absence of a buffer (dashed line). Also shown in Figure S5 are the experimentally recorded pH values for the anode effluent samples from Na_2SO_4 and KNO_3 electrolysis. The experimentally recorded pH values for the KNO_3 anode effluent are in good agreement with the modeled curve in the absence of a buffer, consistent with high anode current utilization (Fig. S4b) and the fact that KNO_3 doesn't exhibit any buffering capacity in the pH range of these experiments because the pK_a of HNO_3 is -1.38.[6] On the other hand, the experimental pH measurements for the Na_2SO_4 anode effluent samples are in good agreement with the modeled pH curve that includes the buffering effect of the sulfate anions. Figure S5 thus provides strong evidence that the difference in anode effluent pH between KNO_3 and Na_2SO_4 electrolysis is due to buffering by SO_4^{2-}.

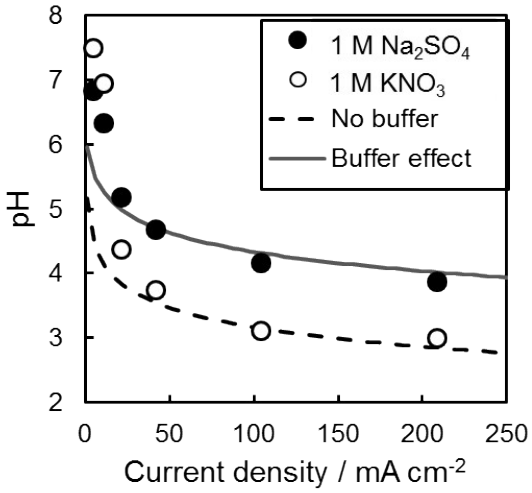

Figure S5: Zoomed-in view of the modeled (dashed and solid lines) and experimental (solid and open circles) curves of pH vs. operating current density for the acidic anode effluent during electrolysis of 1 M Na_2SO_4 or 1 M KNO_3. The experimental data points correspond to those already provided in Figure 3c, where full experimental details are given. The modeled curve without a buffer effect (dashed line) is based on Equation (5) from the main article, while the modeled curve accounting for the buffering effect of the sulfate anion (solid line) was computed as described in the text.

VI. Maximum Achievable Acid and Base Concentrations for a Single Cell

Figure S6 shows the maximum achievable concentrations of acid ($[H^+]$) and base ([OH-]) that could be produced from electrolysis of brine with an initial pH of 7 using a single membraneless flow cell as a function of current density and electrolyte velocity (u). The curves in Figure S6 were calculated using Equation (3) for n= 1 mole e- per mole H^+ and OH^-, and assuming that the coulombic efficiency or current utilization is ξ =100%. For each curve, u was specified and set equal to $u = A/(\nu/2)$ in Equation (3), where A is the area of a single electrode and ν is the total inlet volumetric flow rate.

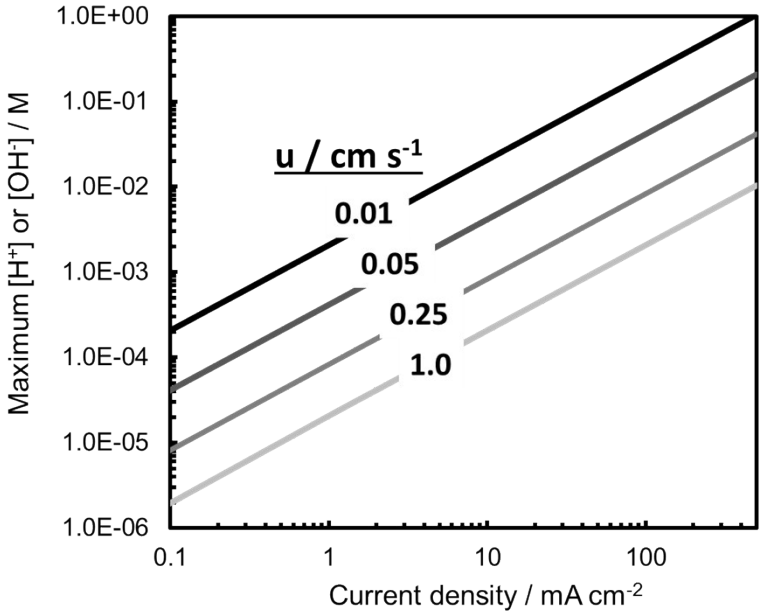

Figure S6: Maximum effluent concentrations modeled based on Equation (3) of the main text as a function of current density and fluid velocity (u=2·A/ν) for a single membraneless electrolysis cell assuming n= 1 e-/mole H^+/OH^- and a current utilization of ξ=100% at both the anode and cathode.

VII. ESI References

1 R. H. Stokes, *Trans. Faraday Soc.*, 1949, **45**, 612–624.

2 M. M. Marcos-arroyo, M. K. Khoshkbarchi and J. H. Vera, *J. Solution Chem.*, 1996, **25**, 983–1000.

3 N. Fujishiro, J. Hatae and H. Kawata, *Comput. Biol. Med.*, 1994, **24**, 221–228.
4 W. M. Haynes, T. J. Bruno and D. R. Lide, Eds., *CRC Handb. Chem. Phys.*, 2017, 5–87.
5 K. H. Tan, *Principles of Soil Chemistry*, CRC Press, 2010.
6 J. A. Dean, Ed., *Lange's Handbook of Chemistry*, McGraw-Hill Book Co., New York, NY, 13 Ed., 1985.